Chemistry Research Journal, 2022, 7(4):14-35

Available online www.chemrj.org

Research Article

ISSN: 2455-8990
CODEN(USA): CRJHA5

On the relationships between electronic structure and 5-HT_{2A}, 5-HT_{2C} and D_2 receptor affinities in a group of 2-aryl tryptamines. A DFT study

Juan S. Gómez-Jeria[1,2]*, Lilian Olarte-Lezcano[1]

[1]Quantum Pharmacology Unit, Department of Chemistry, Faculty of Sciences, University of Chile. Las Palmeras 3425, Santiago 7800003, Chile
[2]Glowing Neurons Group, CP 8270745 Santiago, Chile
Corresponding author: facien03chile.cl

Abstract 2-aryl tryptamines, hallucinogens, serotonin 5-HT_{2A} receptor, serotonin 5-HT_{2C} receptor, dopamine D_2 receptor, Klopman-Peradejordi-Gómez method, QSAR, receptor affinity, drug-receptor interaction, KPG method, alkyl interactions, hydrogen bond formation, MO-MO interactions.

Keywords 5-HT_{2A}, 5-HT_{2C}, D_2, DFT study

Introduction

For several decades, this Unit has explored the relationship between electronic structure and receptor affinity [1-12]. Initially, research focused on serotonin receptors but later it was extended to other receptors [13-34]. In recent years, international pharmacological research has focused on molecules that can interact with more than one receptor at the same time. They are known as multi-target drugs. Their paramount importance is shown with the following example.

Schizophrenia (SP) is a complex disease affecting around 1% of people. The efficacy of the new multitarget drugs in alleviating the symptoms of schizophrenia results not only from their affinity for dopamine D_2 receptor but also for serotonin receptors. The dopamine D_2 receptor is still the main target for the new compounds but also other dopamine receptors, mainly D_3, and serotonin 5-HT_{1A} and 5-HT_{2A} receptors are of great interest. The activation of the 5-HT_{1A} receptor in the frontal cortex will increase the functions of the mesocortical dopamine pathway, improving the negative symptoms and cognitive deficits in patients with SP. An inverse agonist of the 5-HT_{2A} receptor could counteract an excessive D_2 receptor blockade, easing extrapyramidal effects and increasing the efficacy against negative symptoms. In summary, combining D_2/D_3 antagonism, 5-HT_{1A} receptor agonism, and 5-HT_{2A} receptor antagonism showed to be favorable in the management of SP. It is worth to mention that the simultaneous D_2 receptor and 5-HT_{1A} activation might be advantageous in Parkinson disease therapy because the 5-HT_{1A} receptor stimulation might decrease the dyskinetic side effects induced by D_2 receptor activation.

Recently we began to carry out studies on multitarget molecules interacting with dopamine and serotonin receptors [35, 36]. In this paper, we present the results of a study of the relationships between the electronic structure and the 5-HT_{2A}, 5-HT_{2C} and D_2 receptor affinities in a group of 2-aryl tryptamines. We expect to provide some useful results that can be of interests to experimentalists.

Methods, Models and Calculations

The method [37]

To carry out this study we employed the so-called Klopman-Peradejordi-Gómez (KPG) formal method [38-47]. It relates a biological activity (BA) with the electronic structure of the molecule through a linear relationship. The actual version includes twenty local atomic reactivity indices per atom. Then, for some biological activity, we have:

$$\log(BA)=a+b\log\left(M_D\right)+\sum_{o=1}^{subs}\rho_o+\sum_{i=1}^{Z}\left[e_iQ_i+f_iS_i^E+s_iS_i^N\right]+$$
$$+\sum_{i=1}^{Z}\sum_{m=(HOMO-2)*,i}^{(HOMO)*,i}\left[h_i\left(m\right)F_i(m*)+j_i\left(m\right)S_i^E\left(m*\right)\right]+$$
$$+\sum_{i=1}^{Z}\sum_{m'=(LUMO)*,i}^{(LUMO+2)*,i}\left[r_i\left(m'\right)F_i(m'*)+t_i\left(m'\right)S_i^N\left(m'*\right)\right]+$$
$$+\sum_{i=1}^{Z}\left[g_i\mu_i^*+k_i\eta_i^*+o_i\omega_i^*+z_i\zeta_i^*+w_jQ_i^{*,max}\right] \quad (1)$$

where a, b, e_i, f_i, s_i $h_i(m)$, $j_i(m)$, $r_i(m')$, $t_i(m')$, g_i, k_i, o_i, z_i and w_i are constants to be determined, M_D is the mass of the drug and ρ_o is the orientational effect of the o-th substituent. Q_j is the net charge of the atom j. S_j^E and S_j^N are, respectively, the total atomic electrophilic and the total atomic nucleophilic superdelocalizabilities of atom j. $F_j(m)$ and $F_j(m')$ are, respectively, the electron populations (or Fukui indices) of the occupied (m) and vacant (m′) Local Molecular Orbitals (OMs) localized on atom j. $S_j^E(m)$ is the electrophilic superdelocalizability of the local occupied OM m localized on atom j.

The last terms of Eq. 1, derived within the Hartree-Fock scheme by one of the authors (J.S. G.-J.), are: μ_j the local atomic electronic chemical potential of atom j, η_j the local atomic hardness of the atom j, ω_j the local atomic electrophilicity of atom j, ς_j the local atomic softness of the atom j and Q_j^{max} (the maximum amount of electronic charge that atom j can accept) [45]. They are not the local indices derived in Density Functional Theory because in our case they have the same units that the global equivalents (eV and not eV×e). The molecular orbitals carrying an asterisk are the Local Molecular Orbitals (LMO) of each atom. For atom p, the LMOs of p are all the molecular MOs having an electron population greater than 0.01e on p. Here, we have included the three highest occupied local MOs and the three lowest empty local MOs of each atom. More local MOs may be included in Eq. 1 if necessary. A mandatory condition that the linear system of equations 1 must satisfy to be solved is that each equation must have the same number of terms. This condition is satisfied only by selecting a set of atoms common to all the molecules. This is called the common skeleton. The number of atoms of this common skeleton defines the index Z of Eq. 1. The second mandatory condition is that we must have at least the same number of equations than the total number of indices of the common skeleton and the other terms of Eq. 1. As no paper publishes data fulfilling this condition, we use linear multiple regression analysis (LMRA) to detect those indices associated with the variation of the values of the biological activity. This method has produced excellent results for many biological activities and receptors.

Selection of molecules and activities

The selected biological activities were the binding affinities for serotonin (5-HT_{2A} and 5-HT_{2A}) and dopamine (D_2) receptors of sixteen molecules from a paper of Stevenson et al. [48]. All data is shown in Table 1 and Fig. 1.

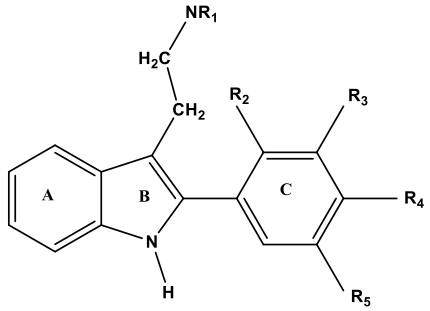

Figure 1: 2-aryl tryptamines

Table 1: 2-aryl tryptamines and their receptor binding affinities

Mol.	Orig.	NR_1	R_2	R_3	R_4	R_5	$\log(K_i)$ 5-HT_{2A}	$\log(K_i)$ 5-HT_{2C}	$\log(K_i)$ D_2
1	3	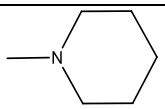	H	H	H	H	0.41	2.43	2.95
2	14	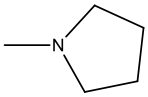	H	H	H	H	0.95	2.41	---
3	15	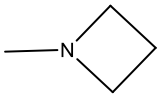	H	H	H	H	1.64	---	---
4	16	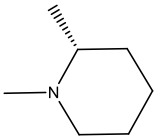	H	H	H	H	-0.74	1.56	1.32
5	17	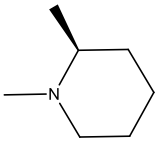	H	H	H	H	0.60	2.36	2.46
6	18	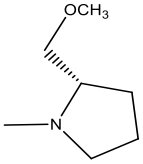	H	H	H	H	-0.59	1.46	1.96
7	21	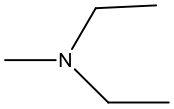	H	H	H	H	0.45	2.20	---
8	22	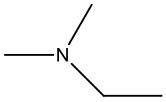	H	H	H	H	-0.85	1.04	1.93
9	25	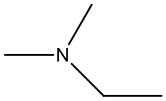	H	H	Cl	H	0.54	1.56	2.40
10	26	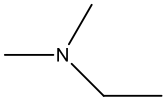	H	H	CN	H	0.41	2.20	0.38

11	27	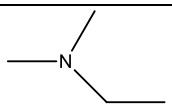	H	H	F	H	-0.37	1.49	1.23
12	28	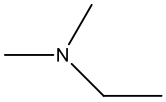	F	H	H	H	-0.52	1.48	2.18
13	29	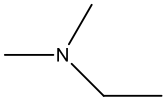	H	F	H	H	-1.10	0.92	1.83
14	30	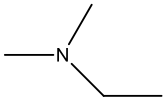	H	NO_2	H	H	-0.85	1.56	1.59
15	31	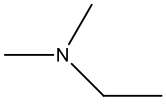	H	CF_3	H	H	-0.89	1.08	1.23
16	32	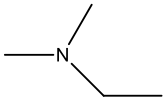	H	CF_3	H	CF_3	-0.72	1.18	2.27

The next figures show the histogram of frequencies and the Box-Whiskers plot of values with median and quartile values for the three sets of data.

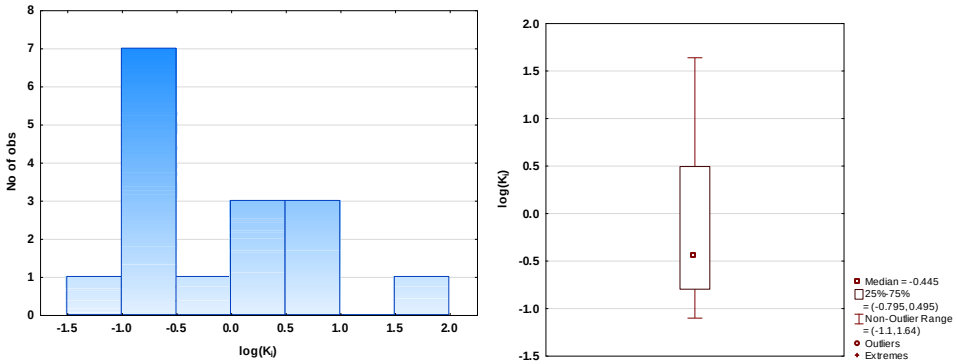

Figure 2: h5-HT_{2A} receptor data. Left. Histogram of frequencies. Right. Box-Whiskers plot

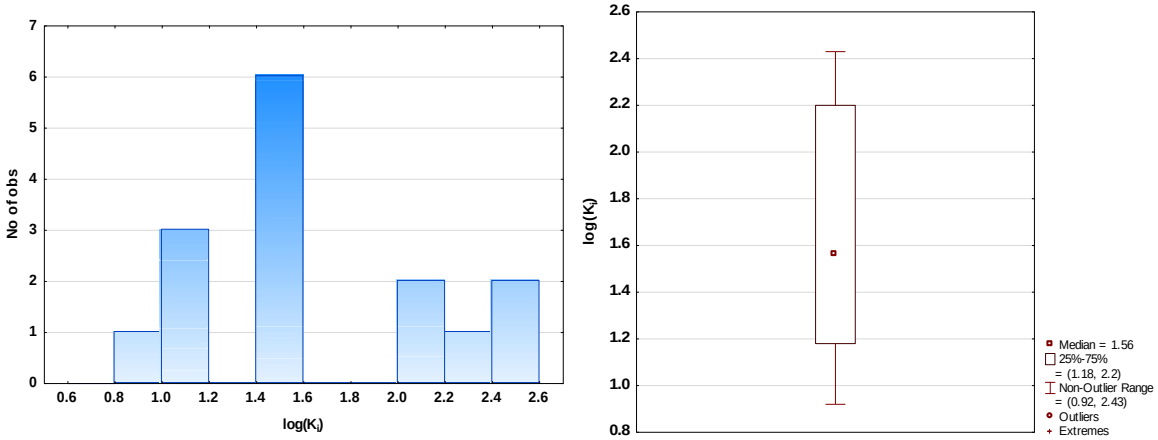

Figure 3: h5-HT_{2C} receptor data. Left. Histogram of frequencies. Right. Box-Whiskers plot

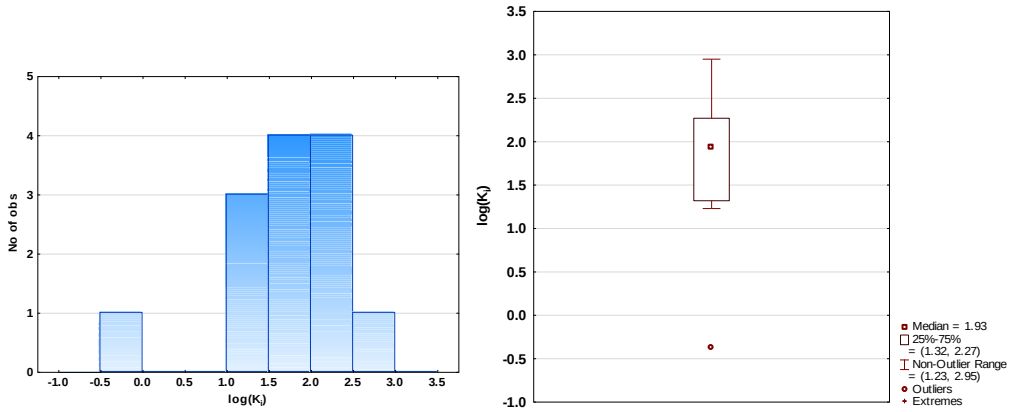

Figure 4: D_2 receptor data. Left. Histogram of frequencies. Right. Box-Whiskers plot

Electronic structure calculations

The electronic structure of all molecules was calculated with the Density Functional Theory (DFT) at the B3LYP/6-31g(d,p) level after full geometry optimization. The Gaussian 16 collection of programs was employed [49]. All the information to calculate the numerical values for the local atomic reactivity indices was obtained with the D-Cent-QSAR software [50]. All electron populations smaller than or equal to 0.01e were considered as being zero. Negative electron populations or populations greater than 2.0 coming from Mulliken Population Analysis were corrected [51]. The Statistica software was used for LMRA [52]. The common skeleton used here is shown in Fig. 5.

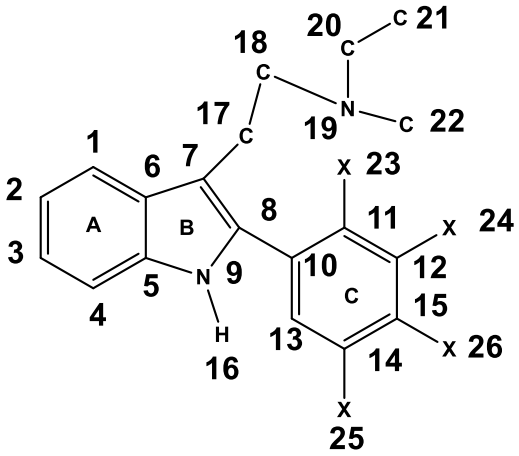

Figure 5: Common skeleton numbering

Results

Results for the h5-HT_{2A} receptor affinity

The best equation obtained is:

$$\log(K_i)=-29.71+273.20s_{20}+0.37S_{24}^{N}(LUMO+1)^{*}-13.36Q_{20}+ \\ +3.80S_{4}^{E}(HOMO)^{*}+7.08S_{15}^{E}(HOMO-1)^{*} \quad (2)$$

with n=16, R=0.97, R^2=0.95, adj-R^2=0.92, F(5,10)=36.161 (p<0.00000) and SD=0.23. No outliers were detected and no residuals fall outside the ±2σ limits. Here, s_{20} is the local atomic softness of atom 20, $S_{24}^{N}(LUMO+1)^{*}$ is the nucleophilic superdelocalizability of the second lowest empty local MO of atom 24, Q_{20} is the net charge of atom 20, $S_4^{E}(HOMO)^{*}$ is the electrophilic superdelocalizability of the highest occupied local MO of atom 4 and $S_{15}^{E}(HOMO-1)^{*}$ is the electrophilic superdelocalizability of the second highest occupied local MO of atom 15. Tables 2 and 3 show the beta coefficients, the results of the t-test for significance of coefficients and the matrix of

squared correlation coefficients for the variables of Eq. 2. There are no significant internal correlations between independent variables. Figure 6 displays the plot of observed *vs.* calculated $\log(K_i)$.

Table 2: Beta coefficients and t-test for significance of coefficients in Eq. 2

	Beta	t(10)	p-level
s_{20}	1.02	11.19	0.000001
S_{24}^N(LUMO+1)*	0.61	8.03	0.00001
Q_{20}	-0.64	-6.44	0.00007
S_4^E(HOMO)*	0.43	4.72	0.0008
S_{15}^E(HOMO-1)*	0.25	2.76	0.02

Table 3: Matrix of squared correlation coefficients for the variables in Eq. 2

	s_{20}	S_{24}^N(LUMO+1)*	Q_{20}	S_4^E(HOMO)*	S_{15}^E(HOMO-1)*
s_{20}	1				
S_{24}^N(LUMO+1)*	0.04	1			
Q_{20}	0.06	0.00	1		
S_4^E(HOMO)*	0.02	0.00	0.31	1	
S_{15}^E(HOMO-1)*	0.20	0.00	0.04	0.00	1

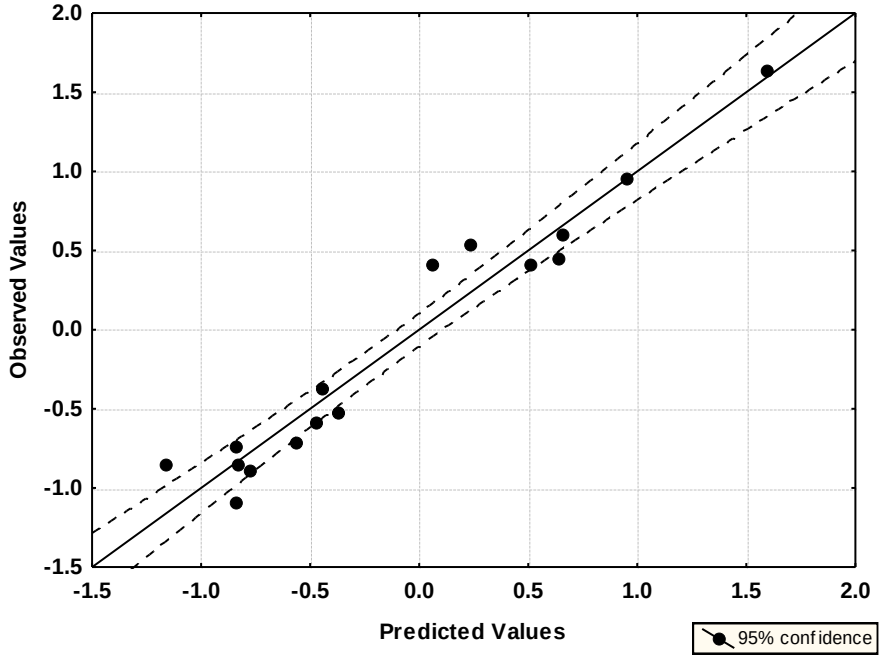

Figure 6: Plot of predicted vs. observed log(K_i) values (Eq. 2). Dashed lines denote the 95% confidence interval

The associated statistical parameters of Eq. 2 indicate that this equation is statistically significant and that the variation of the numerical values of a group of five local atomic reactivity indices of atoms constituting the common skeleton explains about 95% of the variation of $\log(K_i)$. Figure 6, spanning about 2.5 orders of magnitude, shows that there is a good correlation of observed *versus* calculated $\log(K_i)$ values.

Eq. 1 has a linear form but that there are remaining terms containing non-linear expressions that were not considered. For this reason, we need to show, for each case, evidence supporting the hypothesis that a linear model is correct. A good regression analysis minimizes the residuals and it is expected that they be distributed as in a cloud showing no definite pattern or slope, centered (more or less) along of the horizontal axis in a plot of predicted values vs. residuals scores. A random pattern shows that the use of a linear model is correct. The plot of residuals versus deleted residuals shows the stability of the regression coefficients. No large discrepancies should appear between the residuals and the deleted residuals. In addition, we can use a normal probability plot of residuals to evaluate the

normality of the distribution of a variable. If the observed residuals are distributed normally, they should fall on a straight line. Figures 7, 8 and 9 show, respectively, the plot of predicted values vs. residuals scores, the plot of residual vs. deleted residuals and the normal probability plot of residuals.

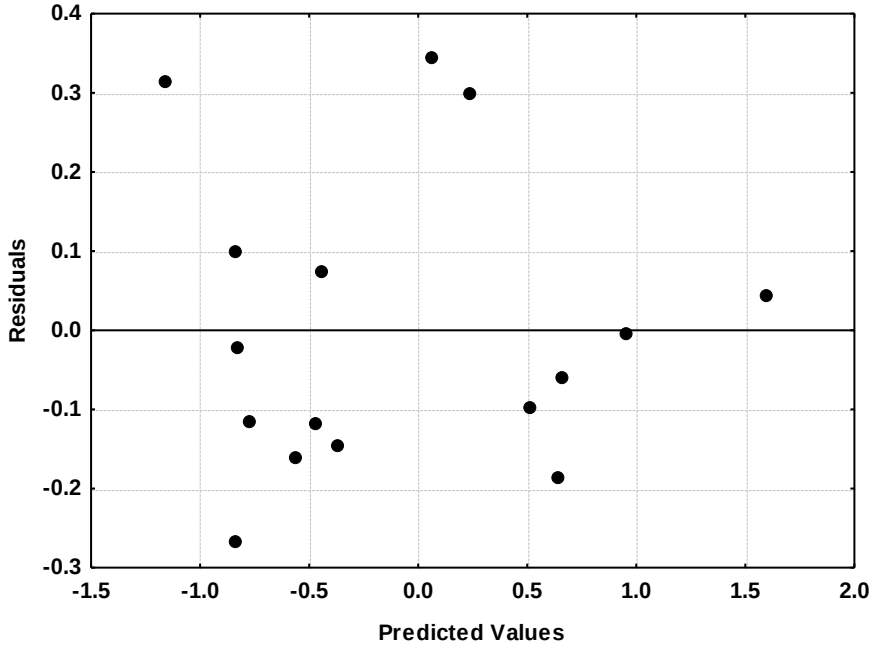

Figure 7: Plot of predicted values vs. residuals scores

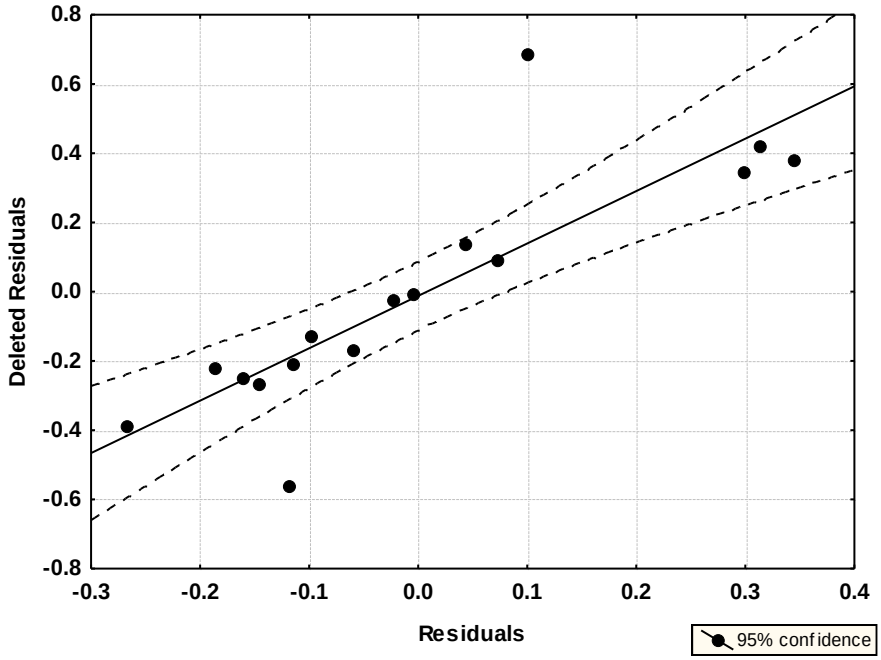

Figure 8: Plot of residual vs. deleted residuals

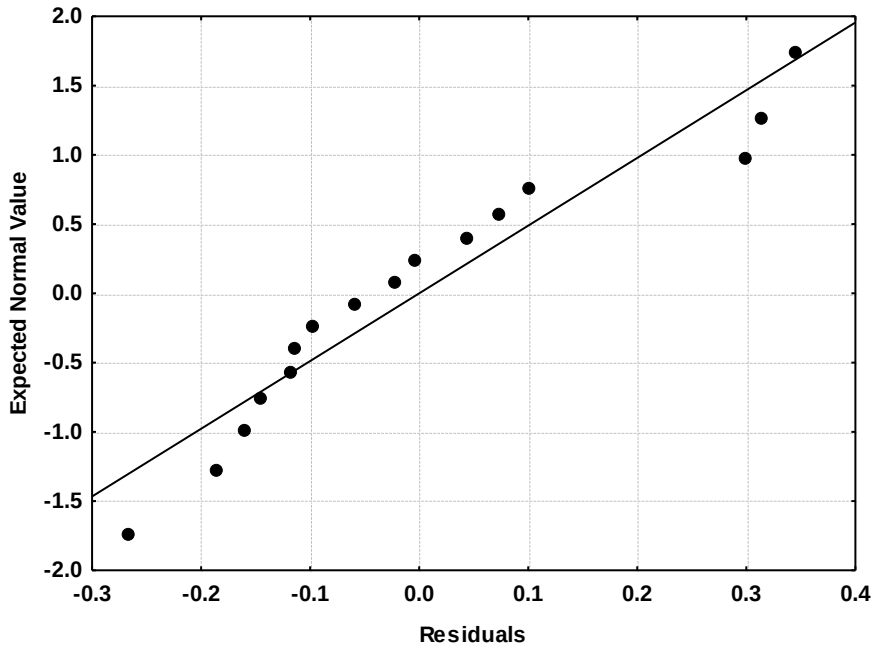

Figure 9: Normal probability plot of residuals

Figures 7 to 9 show that a linear model relating electronic structure with h5-HT_{2A} receptor affinity is a good first approach.

Results for the h5-HT_{2C} receptor affinity

The best equation obtained is:

$$\log(K_i)=44.56-32.03F_{19}(LUMO+2)^{*}+2.43S_{21}^{E}+1.94S_{22}^{E} \quad (3)$$

with n=15, R=0.97, R^2=0.94, adj-R^2=0.92, F(3,11)=56.493 (p<0.00000) and SD=0.15. No outliers were detected and no residuals fall outside the ±2σ limits. Here, $F_{19}(LUMO+2)^{*}$ is the Fukui index (electron population) of the third lowest empty local MO of atom 19, S_{21}^{E} is the total atomic electrophilic superdelocalizability of atom 21 and S_{22}^{E} is the total atomic electrophilic superdelocalizability of atom 22. Tables 4 and 5 show the beta coefficients, the results of the t-test for significance of coefficients and the matrix of squared correlation coefficients for the variables of Eq. 3. There are no significant internal correlations between independent variables (Table 5). Figure 10 displays the plot of observed *vs.* calculated $\log(K_i)$ values.

Table 4: Beta coefficients and t-test for significance of coefficients in Eq. 3

Var.	Beta	t(11)	p-level
$F_{19}(LUMO+2)^{*}$	-0.70	-9.29	0.000002
S_{21}^{E}	0.39	4.85	0.0005
S_{22}^{E}	0.34	4.21	0.001

Table 5: Matrix of squared correlation coefficients for the variables in Eq. 3.

	$F_{19}(LUMO+2)^{*}$	S_{21}^{E}	S_{22}^{E}
$F_{19}(LUMO+2)^{*}$	1		
S_{21}^{E}	0.00	1	
S_{22}^{E}	0.02	0.13	1

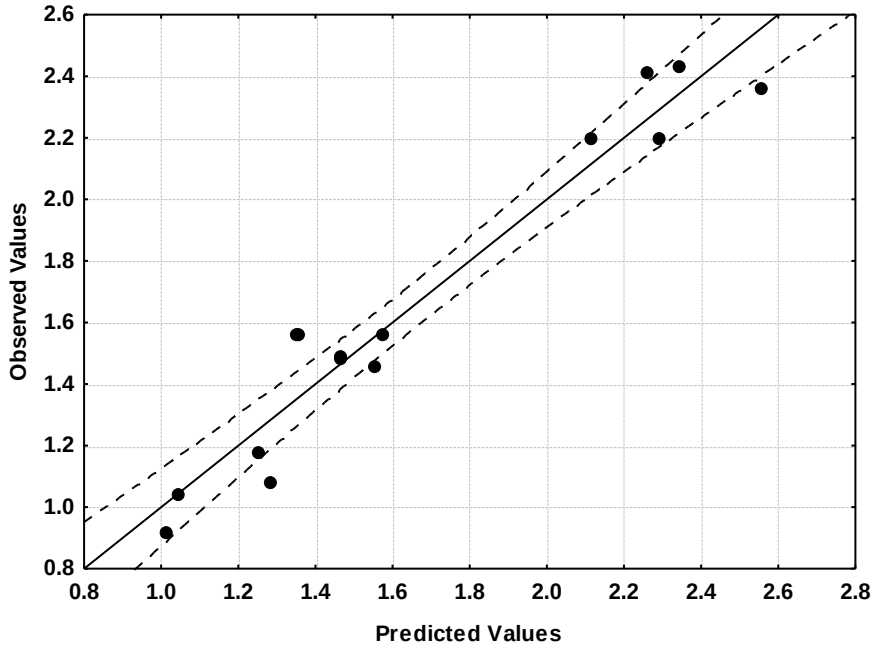

Figure 10. Plot of predicted vs. observed log(K_i) values (Eq. 3). Dashed lines denote the 95% confidence interval

The associated statistical parameters of Eq. 3 indicate that this equation is statistically significant and that the variation of the numerical values of a group of three local atomic reactivity indices of atoms constituting the common skeleton explains about 92% of the variation of log(K_i). Figure 10, spanning about 1.5 orders of magnitude, shows that there is a good correlation of observed *versus* calculated log(K_i) values. Figures 11, 12 and 13 show, respectively, the plot of predicted values vs. residuals scores, the plot of residual vs. deleted residuals and the normal probability plot of residuals.

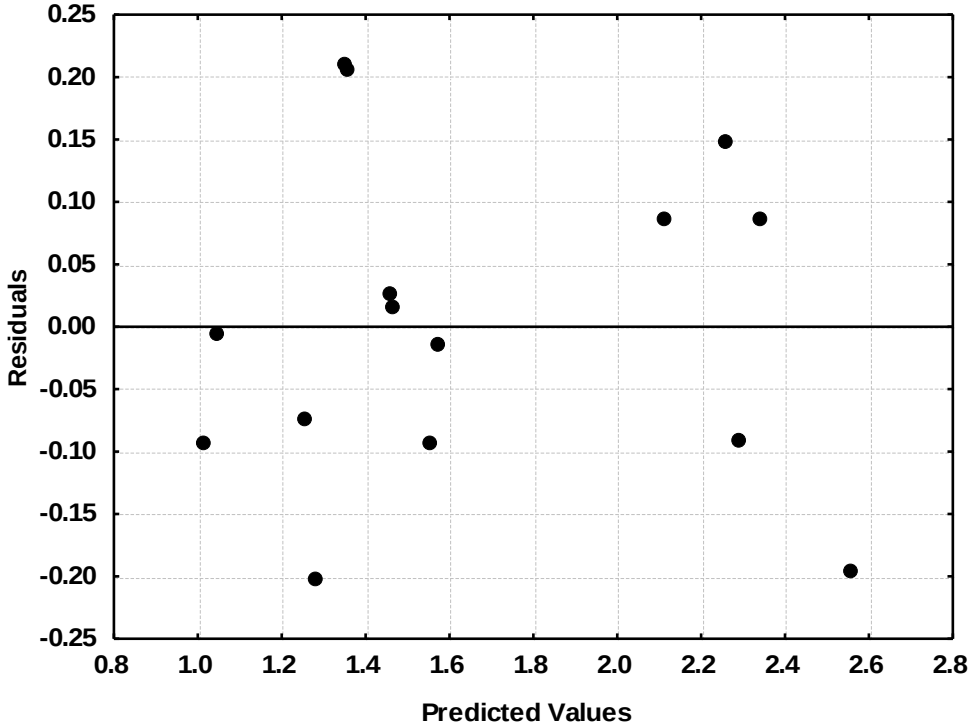

Figure 11: Plot of predicted values vs. residuals scores

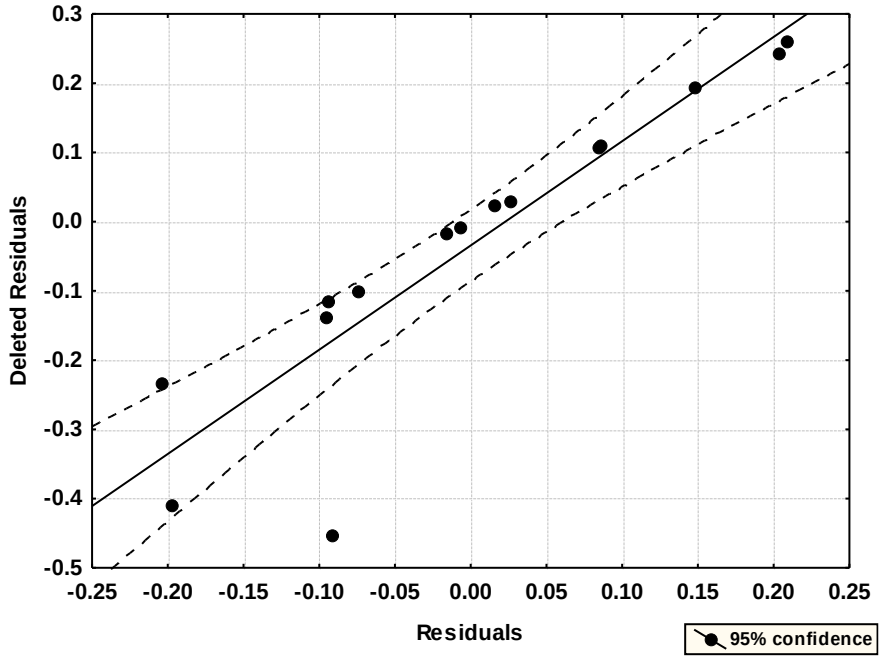

Figure 12: Plot of residual vs. deleted residuals

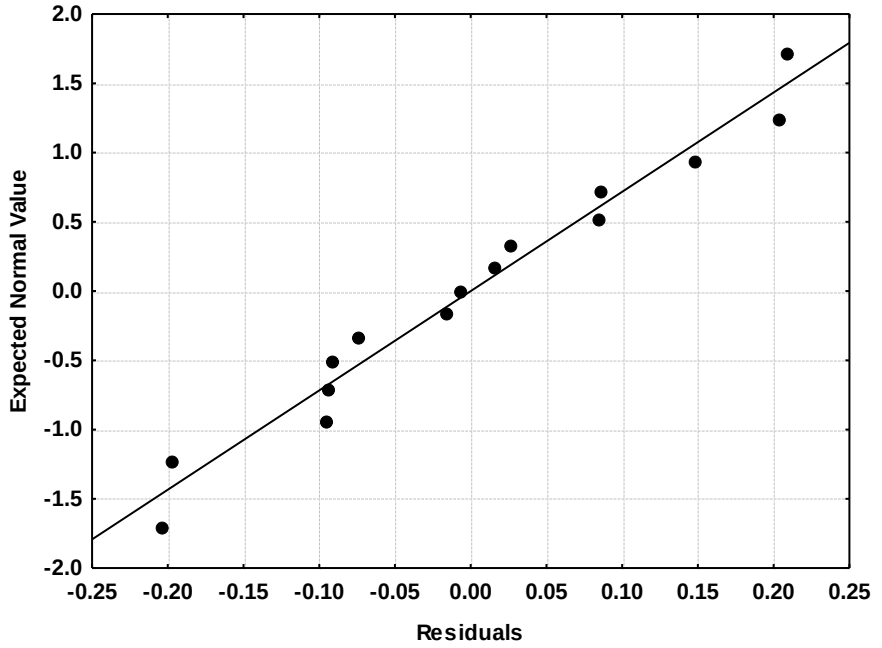

Figure 13: Normal probability plot of residuals

Figures 11 to 13 show that a linear model relating electronic structure with h5-HT_{2C} receptor affinity is a good first approach.

Results for the D_2 receptor affinity

The best equation obtained is:

$$\log(K_i)=10.81-12.88\omega_{21}+0.33S_{14}^{E}(\text{HOMO-2})^*-0.74\eta_{16}+1.74F_5(\text{HOMO-2})^* \quad (4)$$

with n=13, R=0.99, R^2=0.98, adj-R^2=0.97, F(4,8)=114.14 (p<0.00000) and SD=0.13. No outliers were detected and no residuals fall outside the ±2σ limits. Here, , ω_{21} is the local atomic electrophilicity of atom 21, S_{14}^{E}(HOMO-2)* is the electrophilic superdelocalizability of the third highest occupied local MO of atom 14, η_{16} if the local atomic hardness of atom 16 and F_5(HOMO-2)* is the Fukui index of the third highest occupied local MO of atom 5. Tables 6 and 7 show the beta coefficients, the results of the t-test for significance of coefficients and the matrix of squared correlation coefficients for the variables of Eq. 4. There are no significant internal correlations between independent variables (Table 7). Figure 14 displays the plot of observed *vs.* calculated log(K_i).

Table 6: Beta coefficients and t-test for significance of coefficients in Eq. 4

Var.	Beta	t(8)	p-level
ω_{21}	-0.77	-16.24	0.000000
S_{14}^{E}(HOMO-2)*	0.18	3.84	0.005
η_{16}	-0.53	-11.30	0.000003
F_5(HOMO-2)*	0.22	4.54	0.002

Table 7: Matrix of squared correlation coefficients for the variables in Eq. 4

	ω_{21}	S_{14}^{E}(HOMO-2)*	η_{16}	F_5(HOMO-2)*
ω_{21}	1			
S_{14}^{E}(HOMO-2)*	0.00	1		
η_{16}	0.00	0.00	1	
F_5(HOMO-2)*	0.04	0.00	0.03	1

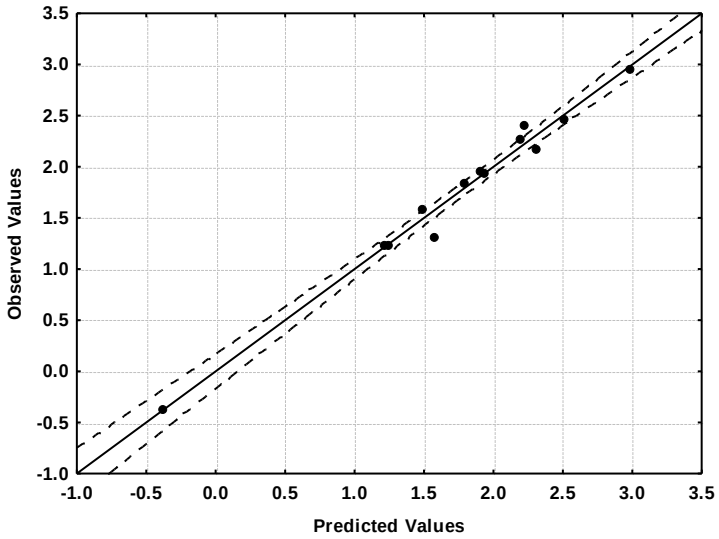

Figure 14: Plot of predicted vs. observed log(K_i) values (Eq. 4). Dashed lines denote the 95% confidence interval

The associated statistical parameters of Eq. 4 indicate that this equation is statistically significant and that the variation of the numerical values of a group of four local atomic reactivity indices of atoms constituting the common skeleton explains about 97% of the variation of log(K_i). Figure 14, spanning about 3.3 orders of magnitude, shows that there is a good correlation of observed *versus* calculated log(K_i) values. Figures 15, 16 and 17 show,

respectively, the plot of predicted values vs. residuals scores, the plot of residual vs. deleted residuals and the normal probability plot of residuals.

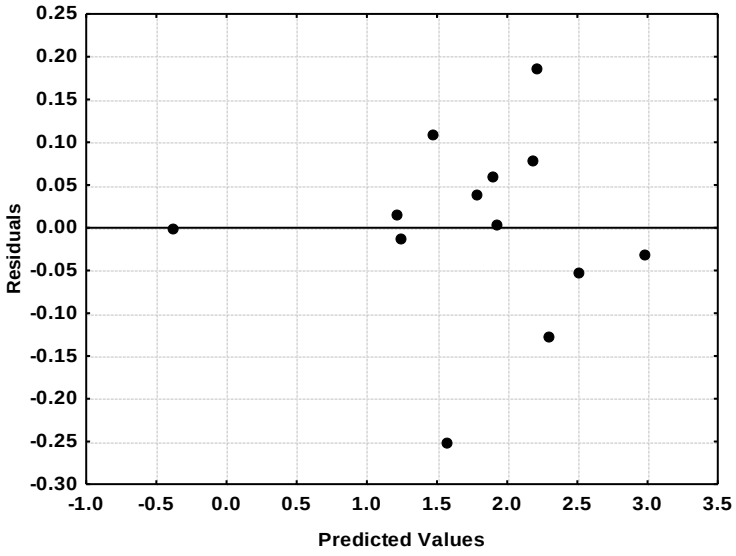

Figure 15: Plot of predicted values vs. residuals scores

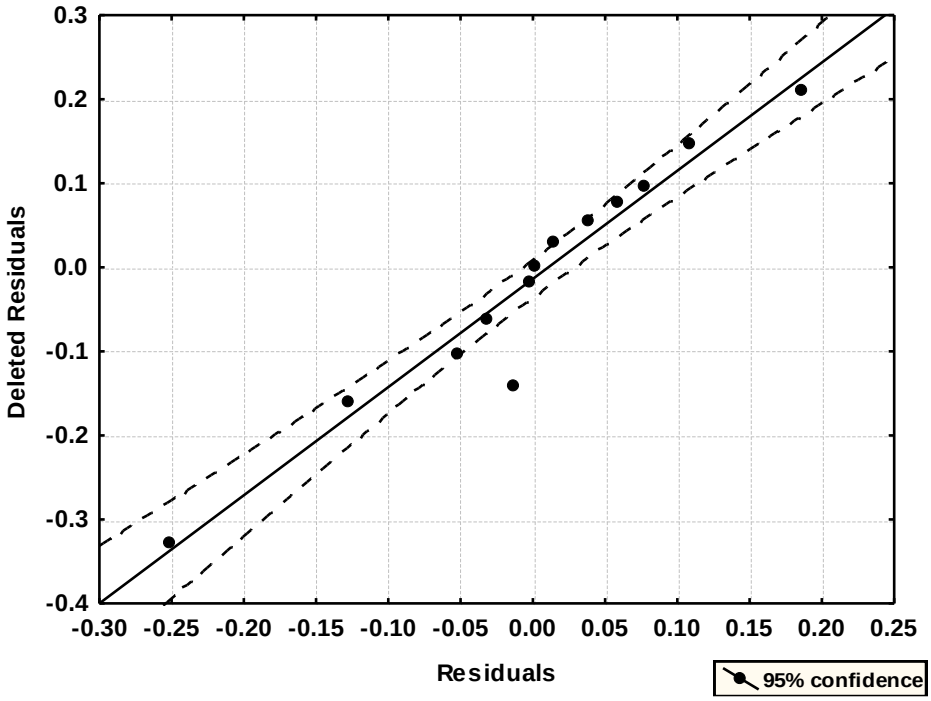

Figure 16: Plot of residual vs. deleted residuals

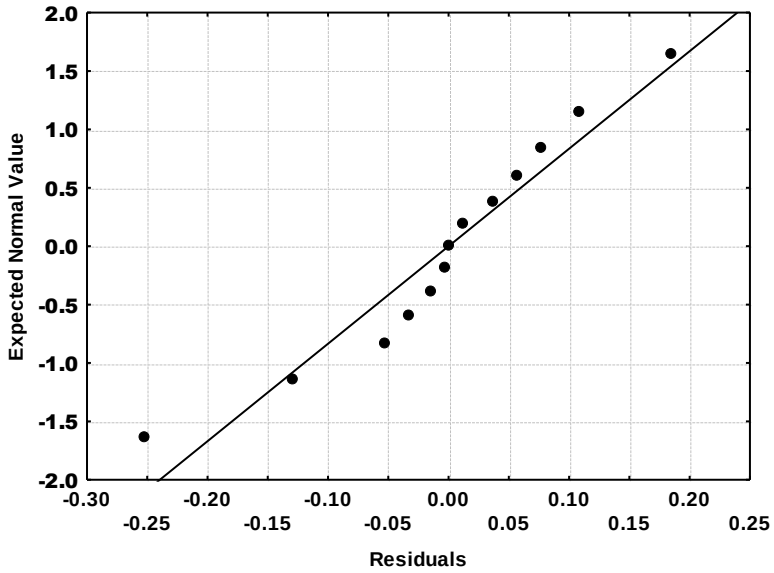

Figure 17: Normal probability plot of residuals

Figures 15 to 17 show that a linear model relating electronic structure with D_2 receptor affinity is a good first approach.

Local Molecular Orbitals

If a local atomic reactivity index of an inner occupied MO (i.e., (HOMO-1)* and/or (HOMO-2)*) or of a higher vacant MO ((LUMO+1)* and/or (LUMO+2)*) appears in an equation, this means that the remaining of the upper occupied MOs (for example, if (HOMO-2)* appears, upper means (HOMO-1)* and (HOMO)*) or the remaining of the empty MOs (for example, if (LUMO+1)* appears, lower means the (LUMO)*) also contribute to the interaction. Their absence in the equation only means that the variation of their numerical values does not account for the variation of the numerical value of the biological property. We work with the hypothesis that any algebraic condition imposed on the numerical values of a reactivity index belonging to an inner occupied local MO or to an upper empty MO of a given atom, also holds for the corresponding local MOs having a lower energy. Tables 8 to 11 show the local molecular orbitals of atoms appearing in Eq. 2-4.

Table 8: Local Molecular Orbitals of atoms 4, 5 and 14

Mol.	A tom 4	Atom 5	Atom 14
1 (82)	78π80π82π- 83π85π86π	77π80π82π- 85π86π87π	77π78π79π- 83π84π85π
2 (78)	75π76π78π- 79π81π82π	73π76π78π- 81π82π83π	73π74π75π- 79π80π81π
3 (74)	72π73π74π- 75π77π78π	72π73π74π- 77π78π79π	69π70π71π- 75π76π77π
4 (86)	82π84π86π- 87π89π90π	84π85π86π- 89π90π91π	81π82π83π- 87π88π89π
5 (86)	82π84π86π- 87π89π90π	84π85π86π- 89π90π91π	81π82π83π- 87π88π89π
6 (94)	92π93π94π- 95π97π98π	92π93π94π- 97π98π99π	89π90π91π- 95π96π97π
7 (79)	75π77π79π- 80π82π83π	77π78π79π- 80π82π83π	74π75π76π- 80π81π82π
8 (75)	71π73π75π-	73π74π75π-	70π71π72π-

	76π78π79π	76π78π79π	76π77π78π
9 (83)	80π81π83π- 84π86π89π	81π82π83π- 84π86π87π	78π79π80π- 84π85π86π
10 (81)	78π79π81π- 82π84π85π	76π79π81π- 82π84π85π	76π77π78π- 82π83π84π
11 (79)	76π77π79π- 80π82π83π	77π78π79π- 80π82π83π	75π76π79π- 80π81π82π
12 (79)	76π77π79π- 80π81π82π	77π78π79π- 80π82π83π	75π76π77π- 80π81π82π
13 (79)	75π77π79π- 80π81π82π	74π77π79π- 80π82π83π	74π75π76π- 80π81π82π
14 (86)	84π85π86π- 88π89π90π	84π85π86π- 88π90π91π	81π82π83π- 87π88π89π
15 (91)	88π89π91π- 92π93π94π	88π89π91π- 92π94π95π	86π87π88π- 92π93π94π
16 (107)	105π106π107π- 108π110π111π	105π106π107π- 108π110π111π	102π103π104π- 108π109π110π

Table 9: Local Molecular Orbitals of atoms 15, 16 and 17

Mol.	Atom 15	Atom 16	Atom 17
1 (82)	79π80π82π- 83π84π85π	55σ57σ66σ- 84σ86σ87σ	78σ81σ82σ- 87σ94σ95σ
2 (78)	75π76π78π- 79π80π81π	51σ55σ62σ- 80σ82σ83σ	73σ77σ78σ- 83σ90σ94σ
3 (74)	70π73π74π- 75π76π77π	51σ52σ57σ- 76σ78σ79σ	70σ72σ74σ- 79σ87σ90σ
4 (86)	82π84π86π- 87π88π89π	51σ57σ59σ- 88σ90σ91σ	82σ85σ86σ- 91σ93σ96σ
5 (86)	84π85π86π- 87π88π89π	58σ59σ72σ- 88σ90σ91σ	81σ85σ86σ- 91σ92σ96σ
6 (94)	92π93π94π- 95π96π97π	63σ64σ65σ- 96σ98σ99σ	88σ93σ94σ- 99σ100σ102σ
7 (79)	76π77π79π- 80π81π82π	55σ56σ58σ- 81σ83σ84σ	75σ78σ79σ- 84σ87σ92σ
8 (75)	72π73π75π- 76π77π78π	52σ54σ56σ- 77σ79σ80σ	71σ74σ75σ- 80σ82σ84σ
9 (83)	80π81π83π- 84π85π86π	58σ60σ62σ- 85σ88σ89σ	78σ82σ83σ- 89σ94σ96σ
10 (81)	78π79π81π- 82π83π84π	54σ55σ58σ- 83σ85σ87σ	78σ80σ81σ- 87σ90σ93σ
11 (79)	76π77π79π- 80π81π82π	54σ56σ58σ- 81σ83σ84σ	74σ78σ79σ- 84σ86σ88σ
12 (79)	76π77π79π- 80π81π82π	55σ56σ60σ- 81σ83σ84σ	75σ78σ79σ- 84σ86σ89σ
13 (79)	76π77π79π- 80π81π82π	55σ57σ59σ- 81σ83σ84σ	75σ78σ79σ- 84σ86σ88σ
14 (86)	83π84π86π- 87π88π89π	59σ60σ62σ- 89σ91σ92σ	83σ85σ86σ- 92σ94σ97σ

15 (91)	88π89π91π- 92π93π94π	62σ63σ64σ- 93σ95σ96σ	88σ90σ91σ- 96σ100σ103σ
16 (107)	104π105π107π- 108π109π110π	75σ76σ80σ- 109σ111σ112σ	75σ76σ80σ- 109σ111σ112σ

Table 10: Local Molecular Orbitals of atoms 19, 20 and 21

Mol.	Atom 19	Atom 20	Atom 21
1 (82)	76σ80σ81σ- 91σ93σ94σ	75σ76σ81σ- 91σ92σ93σ	75σ76σ81σ- 93σ94σ96σ
2 (78)	76σ77σ78σ- 87σ88σ89σ	71σ72σ77σ- 86σ88σ89σ	70σ71σ72σ- 85σ88σ90σ
3 (74)	72σ73σ74σ- 82σ84σ85σ	67σ68σ72σ- 79σ81σ84σ	67σ68σ72σ- 79σ81σ84σ
4 (86)	84σ85σ86σ- 94σ98σ99σ	79σ80σ85σ- 95σ96σ97σ	79σ80σ85σ- 95σ96σ99σ
5 (86)	84σ85σ86σ- 94σ99σ100σ	80σ81σ85σ- 94σ96σ97σ	79σ80σ85σ- 94σ99σ100σ
6 (94)	87σ93σ94σ- 105σ107σ109σ	87σ93σ94σ- 106σ107σ108σ	87σ93σ94σ- 103σ104σ105σ
7 (79)	77σ78σ79σ- 84σ92σ93σ	72σ73σ78σ- 87σ89σ91σ	72σ73σ78σ- 88σ92σ95σ
8 (75)	73σ74σ75σ- 80σ87σ88σ	68σ69σ74σ- 84σ85σ87σ	67σ69σ74σ- 84σ86σ87σ
9 (83)	81σ82σ83σ- 89σ95σ97σ	75σ76σ82σ- 92σ93σ95σ	75σ76σ82σ- 94σ97σ100σ
10 (81)	79σ80σ81σ- 95σ96σ97σ	73σ75σ80σ- 91σ93σ96σ	73σ75σ80σ- 88σ92σ94σ
11 (79)	77σ78σ79σ- 84σ91σ92σ	72σ73σ78σ- 88σ89σ91σ	72σ73σ78σ- 88σ90σ92σ
12 (79)	77σ78σ79σ- 84σ92σ94σ	72σ73σ78σ- 89σ90σ92σ	72σ73σ78σ- 88σ92σ95σ
13 (79)	77σ78σ79σ- 84σ91σ92σ	72σ73σ78σ- 88σ89σ91σ	72σ73σ78σ– 90σ92σ95σ
14 (86)	83σ85σ86σ- 92σ99σ101σ	76σ77σ85σ– 97σ100σ101σ	76σ77σ85σ– 96σ98σ101σ
15 (91)	88σ90σ91σ- 96σ104σ105σ	84σ85σ90σ– 99σ101σ102σ	84σ85σ90σ- 100σ105σ106σ
16 (107)	104σ106σ107σ- 112σ121σ122σ	104σ106σ107σ- 112σ121σ122σ	104σ106σ107σ- 112σ121σ122σ

Table 11: Local Molecular Orbitals of atoms 22 and 24

Mol.	Atom 22	Atom 24
1 (82)	75σ76σ81σ- 92σ94σ96σ	56σ68σ69σ- 88σ89σ90σ
2 (78)	71σ72σ77σ- 87σ88σ89σ	62σ64σ65σ- 84σ85σ86σ
3 (74)	67σ68σ72σ- 79σ81σ82σ	62σ63σ64σ- 80σ81σ82σ
4 (86)	79σ80σ85σ- 94σ96σ97σ	72σ73σ74σ- 92σ93σ95π
5 (86)	81σ85σ86σ- 96σ97σ98σ	72σ73σ75σ- 91σ92σ93σ

6 (94)	87σ93σ94σ-101σ105σ106σ	76σ78σ81σ- 99σ100σ101σ
7 (79)	72σ73σ78σ- 85σ90σ91σ	57σ65σ68σ- 84σ85σ86σ
8 (75)	67σ69σ74σ- 86σ87σ88σ	62σ63σ64σ- 80σ81σ82σ
9 (83)	74σ76σ82σ- 93σ95σ97σ	66σ67σ68σ- 87σ88σ90σ
10 (81)	72σ75σ80σ- 92σ94σ95σ	64σ65σ74σ- 86σ88σ90σ
11 (79)	71σ73σ78σ- 90σ91σ92σ	63σ68σ69σ- 84σ85σ86σ
12 (79)	72σ73σ78σ- 87σ90σ92σ	62σ66σ67σ- 84σ85σ87σ
13 (79)	71σ73σ78σ- 85σ90σ91σ	72π74π76π- 81π82π84π
14 (86)	76σ77σ85σ- 96σ98σ99σ	78π79σ80σ- 87π88π89π
15 (91)	84σ85σ90σ- 97σ102σ104σ	78σ79σ87π- 92π93π96π
16 (107)	100σ101σ106σ-113σ117σ118σ	92σ94σ103π-108π109π110π

Discussion

Discussion of the h5-HT_{2A} receptor affinity results

Table 2 shows that the importance of variables in Eq. 2 is s_{20}>>Q_{20} ~ S_{24}^{N}(LUMO+1)*>> S_4^{E}(HOMO)*> S_{15}^{E}(HOMO-1)*. The local atomic softness always has positive numerical values, net charges may have negative, zero or positive numerical values, electrophilic superdelocalizabilities always have negative numerical values and nucleophilic superdelocalizabilities may have positive or negative numerical values. With these considerations and with the algebraic analysis of Eq. 2 we can see that a high h5-HT_{2A} receptor affinity is associated with small numerical values for s_{20}, with a positive net charge of atom 20, with large negative values for S_4^{E}(HOMO)* and S_{15}^{E}(HOMO-1)*, and with small positive numerical values for S_{24}^{N}(LUMO+1)*.

Atom 20 is a sp^3 carbon atom (see Fig. 5). All local MOs have a σ character (Table 10). Local $(HOMO)_{20}^{*}$ coincides with the molecular HOMO or (HOMO-1). The local $(LUMO)_{20}^{*}$ is energetically far from the molecular LUMO (i.e., it coincides with upper empty molecular MOs). A high h5-HT_{2A} receptor affinity is associated with small numerical values for s_{20}. The local atomic softness, s_{20}, is defined as:

$$s_{20}^{*} = \frac{1}{\eta_{20}^{*}} \qquad (5)$$

Therefore, enlarging the $(HOMO)_{20}^{*}$-$(LUMO)_{20}^{*}$ energy gap will produce the required values. The best way is by modifying for example the localization of the molecule's HOMO, (HOMO-1) and (HOMO-2) so that they are not localized on atom 20. This will make atom 20 a bad electron donor and probably create a positive net charge on this atom. In this case, we propose that the σ empty MOs of atom 20 are engaged in an alkyl interaction with occupied σ MOs of the site. Note that the just mentioned requirement of a positive net charge for atom 20 coincides with the requirement of Eq. 2.

Atom 24 is the first atom of the substituent bonded to C12 in ring C (see Fig. 5). These atoms are H, F, N (from NO_2) and C (from CF_3). Table 11 shows that $(HOMO)_{24}^{*}$ is energetically far from the molecular HOMO (i.e., $(HOMO)_{24}^{*}$ coincides with inner occupied MOs with large eigenvalues). In the case of $(LUMO)_{24}^{*}$ it coincides with higher empty MOs (such as (LUMO+4) or (LUMO+5)) when the local MO has a σ nature. In the case when $(LUMO)_{24}^{*}$ has a π nature it coincides with the molecular LUMO (molecules 13-16). A high h5-HT_{2A} receptor affinity is associated with small positive numerical values for S_{24}^{N}(LUMO+1)*. Let us remember that:

$$S_{24}^{N}(LUMO+1)^{*} = \frac{F_{24}(LUMO+1)^{*}}{E_{LUMO+1}^{*}} \qquad (6)$$

where F_{24}(LUMO+1)* is the electron population of $(LUMO+1)_{24}^{*}$ and E_{LUMO+1}^{*} is the corresponding eigenvalue. Therefore, the only way to get small positive numerical values is by shifting the $(LUMO+1)_{24}^{*}$ energy upwards, making this atom a bad electron acceptor. This suggests that atom 24 could be interacting with an electron-deficient center. Considering that we have some atoms with a π $(LUMO+1)_{24}^{*}$ and others with a σ $(HOMO)_{24}^{*}$ we have two possibilities. One is to find a common kind of interaction for both kind of MOs and the other is to suggest the existence of more than one site. Alkyl and/or π-alkyl interactions are good candidates for these interactions.

Atom 4 is a sp^2 carbon atom in ring A (see Fig. 5). A high h5-HT_{2A} receptor affinity is associated with large negative values for S_4^E(HOMO)*. Table 8 shows that $(HOMO)_4^*$ has a π character in all molecules and that it coincides with the molecular HOMO. Large negative values are obtained by shifting upwards the $(HOMO)_4^*$ energy making this atom a better electron donor. This immediately suggests that atom 4 is engaged in π-π interactions with empty π MOs of the site.

Atom 15 is a sp^2 carbon atom in ring C (see Fig. 5). A high h5-HT_{2A} receptor affinity is associated with large negative values for S_{15}^E(HOMO-1)*. Based on a similar analysis carried out for atom 4, it is suggested that atom 15 is also engaged in π-π interactions with empty π MOs of the site. All the suggestions are displayed in the partial 2D pharmacophore of Fig. 18.

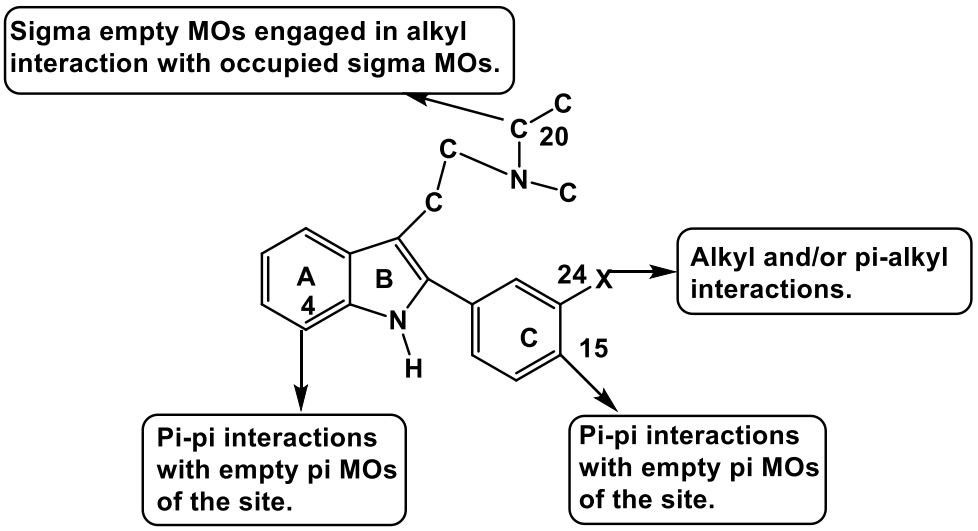

Figure 18: Partial 2D pharmacophore for h5-HT_{2A} receptor affinity

Discussion of the h5-HT_{2C} receptor affinity results

Table 4 shows that the importance of variables in Eq. 3 is F_{19}(LUMO+2)* >> S_{21}^E ~ S_{22}^E.

The algebraic analysis of Eq. 3 shows that a high h5-HT_{2C} receptor affinity is associated with large numerical values for F_{19}(LUMO+2)* and large negative numerical values for S_{21}^E and S_{22}^E.

Atom 19 is the nitrogen atom in the side chain (see Fig. 5). All local MOs have a σ nature (Table 10). $(HOMO)_{19}^*$ coincides with the molecular HOMO and $(LUMO)_{19}^*$ with empty molecular MOs close to the LUMO. A high h5-HT_{2C} receptor affinity is associated with large numerical values for F_{19}(LUMO+2)*. This suggests that this atom is facing an electron-rich center and it is interacting through its empty sigma MOs. A second possibility is that N19 participates in an hydrogen bond of the N19....H-O kind. Actually, we have not enough information to select one of these options.

Atom 21 is a sp^3 carbon atom (see Fig. 5). All local MOs have a σ nature (Table 10). A high h5-HT_{2C} receptor affinity is associated with large negative numerical values for S_{21}^E. Large negative values are obtained by shifting upwards the $(HOMO)_{21}^*$ and other higher occupied MOs eigenvalues, making this atom a better electron donor. We suggest that the σ occupied MOs of atom 21 are engaged in an alkyl interaction with empty σ MOs of the site.

Atom 22 is a sp^3 carbon atom bonded to N19 (Fig. 5). All local MOs have a σ nature (Table 11). A high h5-HT_{2C} receptor affinity is associated with large negative numerical values for S_{22}^E. With the same reasoning used for atom 22, we suggest that the σ occupied MOs of atom 22 are engaged in an alkyl interaction with empty σ MOs of the site. Given the vicinity of atoms 21 and 22, the interaction site could be the same. All the suggestions are displayed in the partial 2D pharmacophore of Fig. 19.

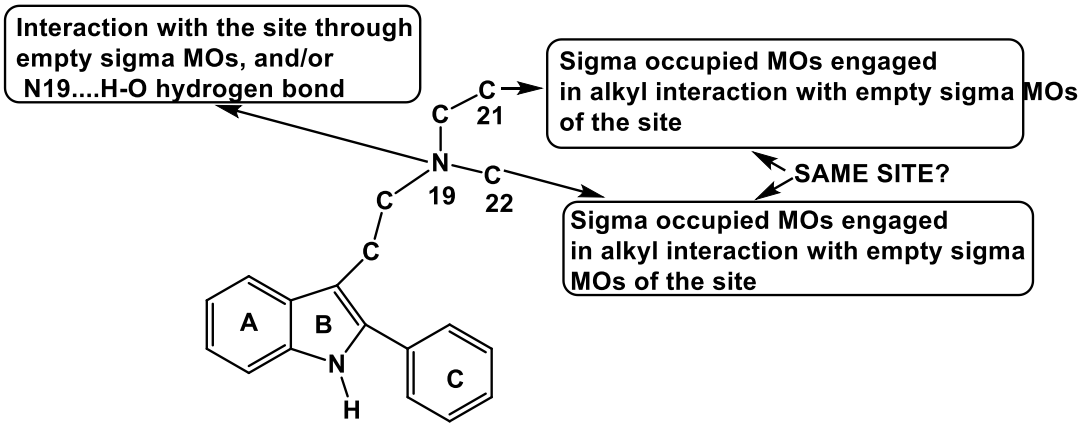

Figure 19: Partial 2D pharmacophore for h5-HT_{2C} receptor affinity

Discussion of the D_2 receptor affinity results

Table 6 shows that the importance of variables in Eq. 6 is $\omega_{21} >> \eta_{16} > F_5(\text{HOMO-2})^* \sim S_{14}^E(\text{HOMO-2})^*$.

The algebraic analysis of Eq. 4 shows that a high D_2 receptor affinity is associated with large positive numerical values for ω_{21} and η_{16}, large negative values for $S_{14}^E(\text{HOMO-2})^*$ and small numerical values for $F_5(\text{HOMO-2})^*$.

Atom 21 is a sp^3 carbon atom (see Fig. 5). All local MOs have a σ nature (Table 10). A high D_2 receptor affinity is associated with large positive numerical values for ω_{21}. The local atomic electrophilic index is defined as:

$$\omega_{21} = \frac{\mu_{21}^2}{2\eta_{21}} \quad (7)$$

As we can see, the numerical values of ω_{21} are always positive. Therefore, we may produce large numerical values by diminishing the value of the local atomic hardness. Table 10 indicates that the easiest way to do this is by localizing the molecular LUMO (or close empty MOs) on atom 21. The other way is by shifting downwards the local $(\text{HOMO})_{21}^*$ (i.e. this local HOMO will correspond to an inner occupied molecular MO). For these reasons, we suggest that atom 21 is involved in an alkyl interaction using the empty sigma MOs.

Atom 16 is a hydrogen atom bonded to N9 in ring B (see Fig. 5). A high D_2 receptor affinity is associated with large numerical values for η_{16}. The local atomic hardness has positive values for this kind of molecules (in metals this local atomic index may have zero or negative values). Table 9 shows that local $(\text{LUMO})_{16}^*$ coincides with the molecular MO close to LUMO and that $(\text{HOMO})_{16}^*$ coincides with inner occupied molecular MOs. The fastest way to obtain large positive numerical values is by changing $(\text{LUMO})_{16}^*$ in such a way that corresponds to a higher empty molecular MO. We may consider atom 16 a positively charged particle devoided of orbital interactions. This immediately suggests the atom 16 is involved in a hydrogen bond N9-H16...X (X=N, O).

Atom 5 is a sp^2 carbon atom shared by rings A and B (see Fig. 5). Table 8 shows that all frontier local MOs have a π nature. $(\text{HOMO})_5^*$ coincides with the molecular HOMO and $(\text{LUMO})_5^*$ coincides with LUMO, (LUMO+1) or (LUMO+2). A high D_2 receptor affinity is associated with small numerical values for $F_5(\text{HOMO-2})^*$. As we made before, we apply this requirement to $F_5(\text{HOMO-1})^*$ and $F_5(\text{HOMO})^*$. Note that N9 is probably attracting electrons from C5. This suggests that atom 5 is engaged in a π-π interaction with the site using the empty π MOs. We do not know if other components of ring A are involved.

Atom 14 is a sp^2 carbon atom in ring C (see Fig. 5). A high D_2 receptor affinity is associated with large negative values for $S_{14}^E(\text{HOMO-2})^*$. These values are obtained by shifting upwards the corresponding eigenvalue. This will shift the $(\text{HOMO-1})_{14}^*$ and $(\text{HOMO})_{14}^*$, making atom 14 prone to interact with its higher occupied local MOs with the empty π MOs of an electron-deficient center. The data in Table 8 suggests a π-π interaction.

All the suggestions are displayed in the partial 2D pharmacophore of Fig. 20.

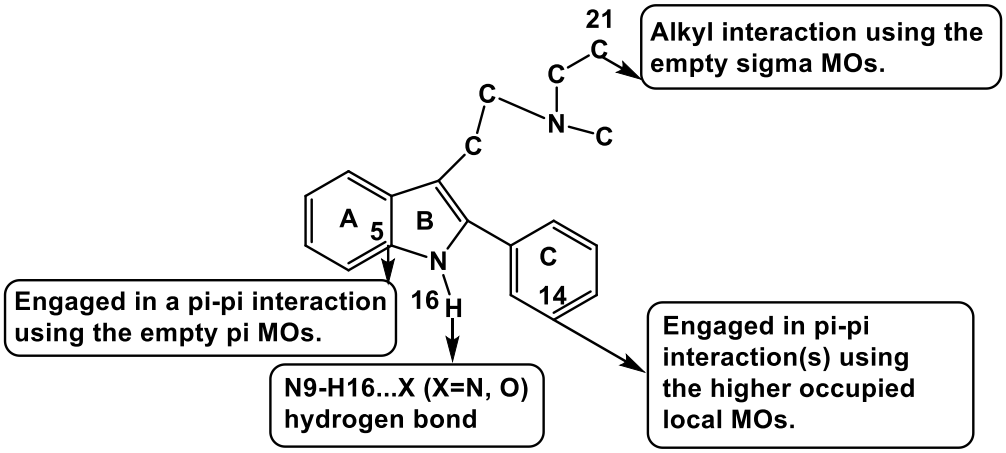

Figure 20: Partial 2D pharmacophore for D_2 receptor affinity

In summary, for the interaction of several 2-aryl tryptamines with 5-HT_{2A}, 5-HT_{2C} and D_2 receptors, we found statistically significant relationships between electronic structure and receptor affinity. This allowed us to suggest specific atom-site interactions such as alkyl interactions of hydrogen bond formation and to build the corresponding pharmacophores.

References

[1]. Gómez-Jeria, J. S.; Morales-Lagos, D. The mode of binding of phenylalkylamines to the Serotonergic Receptor. In *QSAR in design of Bioactive Drugs*, Kuchar, M., Ed. Prous, J.R.: Barcelona, Spain, 1984; pp 145-173.

[2]. Gómez-Jeria, J. S.; Morales-Lagos, D.; Rodriguez-Gatica, J. I.; Saavedra-Aguilar, J. C. Quantum-chemical study of the relation between electronic structure and pA2 in a series of 5-substituted tryptamines. *International Journal of Quantum Chemistry* **1985,** 28, 421-428.

[3]. Gómez-Jeria, J. S.; Morales-Lagos, D.; Cassels, B. K.; Saavedra-Aguilar, J. C. Electronic structure and serotonin receptor binding affinity of 7-substituted tryptamines. *Quantitative Structure-Activity Relationships* **1986,** 5, 153-157.

[4]. Gómez-Jeria, J. S.; Cassels, B. K.; Saavedra-Aguilar, J. C. A quantum-chemical and experimental study of the hallucinogen (±)-1-(2,5-dimethoxy-4-nitrophenyl)-2-aminopropane (DON). *European Journal of Medicinal Chemistry* **1987,** 22, 433-437.

[5]. Gómez-Jeria, J. S.; Robles-Navarro, A. A Density Functional Theory and Docking study of the Relationships between Electronic Structure and 5-HT_{2B} Receptor Binding Affinity in N-Benzyl Phenethylamines. *Der Pharma Chemica* **2015,** 7, 243-269.

[6]. Gómez-Jeria, J. S.; Robles-Navarro, A. A Note on the Docking of some Hallucinogens to the 5-HT_{2A} Receptor. *Journal of Computational Methods in Molecular Design* **2015,** 5, 45-57.

[7]. Gómez-Jeria, J. S.; Robles-Navarro, A. DFT and Docking Studies of the Relationships between Electronic Structure and 5-HT_{2A} Receptor Binding Affinity in N-Benzylphenethylamines. *Research Journal of Pharmaceutical, Biological and Chemical Sciences* **2015,** 6, 1811-1841.

[8]. Gómez-Jeria, J. S.; Robles-Navarro, A. A Quantum Chemical Study of the Relationships between Electronic Structure and cloned rat 5-HT_{2C} Receptor Binding Affinity in N-Benzylphenethylamines. *Research Journal of Pharmaceutical, Biological and Chemical Sciences* **2015,** 6, 1358-1373.

[9]. Gómez-Jeria, J. S.; Abuter-Márquez, J. A Theoretical Study of the Relationships between Electronic Structure and 5-HT_{1A} and 5- HT_{2A} Receptor Binding Affinity of a group of ligands containing an isonicotinic nucleus. *Chemistry Research Journal* **2017,** 2, 198-213.

[10]. Gómez-Jeria, J. S.; Moreno-Rojas, C.; Castro-Latorre, P. A note on the binding of N-2-methoxybenzyl-phenethylamines (NBOMe drugs) to the 5-HT_{2C} receptors. *Chemistry Research Journal* **2018,** 3, 169-175.

[11]. Gómez-Jeria, J. S.; Gatica-Díaz, N. A preliminary quantum chemical analysis of the relationships between electronic structure and 5-HT_{1A} and 5-HT_{2A} receptor affinity in a series of 8-acetyl-7-hydroxy-4-methylcoumarin derivatives. *Chemistry Research Journal* **2019,** 4, 85-100.

[12]. Gómez-Jeria, J. S.; Robles-Navarro, A.; Soza-Cornejo, C. A note on the relationships between electronic structure and serotonin 5-HT_{1A} receptor binding affinity in a series of 4-butyl-arylpiperazine-3-(1*H*-indol-3-yl)pyrrolidine-2,5-dione derivatives. *Chemistry Research Journal* **2021,** 6, 76-88.

[13]. Gómez-Jeria, J. S.; Sotomayor, P. Quantum chemical study of electronic structure and receptor binding in opiates. *Journal of Molecular Structure: THEOCHEM* **1988,** 166, 493-498.

[14]. Gómez-Jeria, J. S.; Parra-Mouchet, J.; Morales-Lagos, D. Electrostatic medium effects upon histamine H 2 receptor activation. *Journal of Molecular Structure: THEOCHEM* **1991,** 236, 201-209.

[15]. Gómez-Jeria, J. S.; Ojeda-Vergara, M. Electrostatic medium effects and formal quantum structure-activity relationships in apomorphines interacting with D_1 and D_2 dopamine receptors. *International Journal of Quantum Chemistry* **1997,** 61, 997-1002.

[16]. Gómez-Jeria, J. S.; Lagos-Arancibia, L. Quantum-chemical structure-affinity studies on kynurenic acid derivatives as Gly/NMDA receptor ligands. *International Journal of Quantum Chemistry* **1999,** 71, 505-511.

[17]. Gómez-Jeria, J. S.; Lagos-Arancibia, L.; Sobarzo-Sánchez, E. Theoretical study of the opioid receptor selectivity of some 7-arylidenenaltrexones. *Boletin de la Sociedad Chilena de Quimica* **2003,** 48, 61-66.

[18]. Gómez-Jeria, J. S.; Gerli-Candia, L. A.; Hurtado, S. M. A structure-affinity study of the opioid binding of some 3-substituted morphinans. *Journal of the Chilean Chemical Society* **2004,** 49, 307-312.

[19]. Gómez-Jeria, J. S.; Soto-Morales, F.; Rivas, J.; Sotomayor, A. A theoretical structure-affinity relationship study of some cannabinoid derivatives. *Journal of the Chilean Chemical Society* **2008,** 53, 1393-1399.

[20]. Gómez-Jeria, J. S. A DFT study of the relationships between electronic structure and peripheral benzodiazepine receptor affinity in a group of N,N-dialkyl-2- phenylindol-3-ylglyoxylamides (Erratum in: J. Chil. Chem. Soc., 55, 4, IX, 2010). *Journal of the Chilean Chemical Society* **2010,** 55, 381-384.

[21]. Bruna-Larenas, T.; Gómez-Jeria, J. S. A DFT and Semiempirical Model-Based Study of Opioid Receptor Affinity and Selectivity in a Group of Molecules with a Morphine Structural Core. *International Journal of Medicinal Chemistry* **2012,** 2012 Article ID 682495, 1-16.

[22]. Gómez-Jeria, J. S. A quantum-chemical analysis of the relationships between hCB2 cannabinoid receptor binding affinity and electronic structure in a family of 4-oxo-1,4-dihydroquinoline-3-carboxamide derivatives. *Der Pharmacia Lettre* **2014,** 6., 95-104.

[23]. Salgado-Valdés, F.; Gómez-Jeria, J. S. A Theoretical Study of the Relationships between Electronic Structure and CB1 and CB2 Cannabinoid Receptor Binding Affinity in a Group of 1-Aryl-5-(1-H-pyrrol-1-yl)-1-H-pyrazole-3-carboxamides. *Journal of Quantum Chemistry* **2014,** 2014 Article ID 431432, 1-15.

[24]. Solís-Gutiérrez, R.; Gómez-Jeria, J. S. A Density Functional Theory study of the relationships between electronic structure and metabotropic glutamate receptor subtype 5 affinity of 2-amino- and 2-halothiazole derivatives. *Research Journal of Pharmaceutical, Biological and Chemical Sciences* **2014,** 5, 1401-1416.

[25]. Gómez-Jeria, J. S.; Valdebenito-Gamboa, J. Electronic structure and docking studies of the Dopamine D_3 receptor binding affinity of a series of [4-(4-Carboxamidobutyl)]-1-arylpiperazines. *Der Pharma Chemica* **2015,** 7, 323-347.

[26]. Gómez-Jeria, J. S.; Valdebenito-Gamboa, J. A Density Functional Study of the Relationships between Electronic Structure and Dopamine D_2 receptor binding affinity of a series of [4-(4-Carboxamidobutyl)]-1-arylpiperazines. *Research Journal of Pharmaceutical, Biological and Chemical Sciences* **2015,** 6, 203-218.

[27]. Gómez-Jeria, J. S.; Garrido-Sáez, N. A DFT analysis of the relationships between electronic structure and affinity for dopamine D_2, D_3 and D_4 receptor subtypes in a group of 77-LH-28-1 derivatives. *Chemistry Research Journal* **2019,** 4, 30-42.

[28]. Gómez-Jeria, J. S.; Sánchez-Jara, B. An introductory theoretical investigation of the relationships between electronic structure and A1, A2A and A3 adenosine receptor affinities of a series of N6-8,9-trisubstituted purine derivatives. *Chemistry Research Journal* **2019,** 4, 46-59.

[29]. Gómez-Jeria, J. S.; López-Aravena, R. A Theoretical Analysis of the Relationships between Electronic Structure and Dopamine D_4 Receptor Affinity in a series of compounds based on the classical D_4 agonist A-412997. *Chemistry Research Journal* **2020,** 5, 1-9.

[30]. Gómez-Jeria, J. S.; Soloaga Ardiles, C. E.; Kpotin, G. A. A DFT Analysis of the Relationships between Electronic Structure and Human κ, δ and μ Opioid Receptor Binding Affinity in a series of Diphenethylamines. *Chemistry Research Journal* **2020,** 5, 32-46.

[31]. Gómez-Jeria, J. S.; Valenzuela-Hueichaqueo, N. J. The relationships between electronic structure and human A_1 adenosine receptor binding affinity in a series of triazolopyridine derivatives. *Chemistry Research Journal* **2020,** 5, 226-236.

[32]. Gómez-Jeria, J. S.; Ibertti-Arancibia, A. A DFT study of the relationships between electronic structure and dopamine D_1 and D_2 receptor affinity of a group of (S)-enantiomers of 11-(1,6-dimethyl-1,2,3,6-tetrahydropyridin-4-yl)-5*H*-dibenzo[b,e][1,4]diazepines. *Chemistry Research Journal* **2021,** 6, 116-131.

[33]. Gómez-Jeria, J. S.; Robles-Navarro, A.; Soto-Martínez, V. Quantum Chemical Analysis of the relationships between electronic structure and dopamine D_1 and D_5 receptor binding affinities in a series of 1-phenylbenzazepines. *Chemistry Research Journal* **2021,** 6, 128-144.

[34]. Gómez-Jeria, J. S.; Ibertti-Arancibia, A.; Olarte-Lezcano, L. A theoretical study of the relationships between electronic structure of 2-aryladenine derivatives and percentage of inhibition of radioligand binding in human A_{2A} and A_{2B} adenosine receptors. *Chemistry Research Journal* **2022,** 7, 1-18.

[35]. Gómez-Jeria, J. S.; Robles-Navarro, A.; Jaramillo-Hormazábal, I. A DFT analysis of the relationships between electronic structure and activity at D_2, 5-HT_{1A} and 5-HT_{2A} receptors in a series of Triazolopyridinone derivatives. *Chemistry Research Journal* **2022,** 7, 6-28.

[36]. Gómez-Jeria, J. S.; Rojas-Candia, V. A DFT Investigation of the Relationships between Electronic Structure and D_2, 5-HT_{1A}, 5-HT_{2A}, 5-HT_6 and 5-HT_7 Receptor Affinities in a group of Fananserin derivatives. *Chemistry Research Journal* **2020,** 5, 37-58.

[37]. The results presented here are obtained from what is now a routinary procedure. For this reason, all papers have a similar general structure. This model contains *standard* phrases for the presentation of the methods, calculations and results because they do not need to be rewritten repeatedly and because the number of possible variations to use is finite. See: Hall, S., Moskovitz, C., and Pemberton, M. 2021. Understanding Text Recycling: A Guide for Researchers. Text Recycling Research Project. Online at textrecycling.org. In.

[38]. Gómez Jeria, J. S. La Pharmacologie Quantique. *Bollettino Chimico Farmaceutico* **1982,** 121, 619-625.

[39]. Gómez-Jeria, J. S. On some problems in quantum pharmacology I. The partition functions. *International Journal of Quantum Chemistry* **1983,** 23, 1969-1972.

[40]. Gómez-Jeria, J. S. The use of competitive ligand binding results in QSAR studies. *Il Farmaco; Edizione Scientifica* **1985,** 40, 299-302.

[41]. Gómez-Jeria, J. S. Modeling the Drug-Receptor Interaction in Quantum Pharmacology. In *Molecules in Physics, Chemistry, and Biology*, Maruani, J., Ed. Springer Netherlands: 1989; Vol. 4, pp 215-231.

[42]. Gómez-Jeria, J. S.; Ojeda-Vergara, M. Parametrization of the orientational effects in the drug-receptor interaction. *Journal of the Chilean Chemical Society* **2003,** 48, 119-124.

[43]. Alarcón, D. A.; Gatica-Díaz, F.; Gómez-Jeria, J. S. Modeling the relationships between molecular structure and inhibition of virus-induced cytopathic efects. Anti-HIV and anti-H1N1 (Influenza) activities as examples. *Journal of the Chilean Chemical Society* **2013,** 58, 1651-1659.

[44]. Gómez-Jeria, J. S. *Elements of Molecular Electronic Pharmacology (in Spanish)*. 1st ed.; Ediciones Sokar: Santiago de Chile, 2013; p 104.

[45]. Gómez-Jeria, J. S. A New Set of Local Reactivity Indices within the Hartree-Fock-Roothaan and Density Functional Theory Frameworks. *Canadian Chemical Transactions* **2013,** 1, 25-55.

[46]. Gómez-Jeria, J. S.; Flores-Catalán, M. Quantum-chemical modeling of the relationships between molecular structure and in vitro multi-step, multimechanistic drug effects. HIV-1 replication inhibition and inhibition of cell proliferation as examples. *Canadian Chemical Transactions* **2013,** 1, 215-237.

[47]. Paz de la Vega, A.; Alarcón, D. A.; Gómez-Jeria, J. S. Quantum Chemical Study of the Relationships between Electronic Structure and Pharmacokinetic Profile, Inhibitory Strength toward Hepatitis C virus NS5B Polymerase and HCV replicons of indole-based compounds. *Journal of the Chilean Chemical Society* **2013,** 58, 1842-1851.

[48]. Stevenson, G. I.; Smith, A. L.; Lewis, S.; Michie, S. G.; Neduvelil, J. G.; Patel, S.; Marwood, R.; Patel, S.; Castro, J. L. 2-Aryl tryptamines: selective high-affinity antagonists for the h5-HT_{2A} receptor. *Bioorganic & medicinal chemistry letters* **2000,** 10, 2697-2699.

[49]. Frisch, M. J.; Trucks, G. W.; Schlegel, H. B.; Scuseria, G. E.; Robb, M. A.; Cheeseman, J. R.; Scalmani, G.; Barone, V.; Petersson, G. A.; Nakatsuji, H.; Li, X.; Caricato, M.; Marenich, A. V.; Bloino, J.; Janesko, B. G.; Gomperts, R.; Mennucci, B.; Hratchian, H. P. *Gaussian 16 16Rev. A.03*, Gaussian: Pittsburgh, PA, USA, 2016.

[50]. Gómez-Jeria, J. S. *D-Cent-QSAR: A program to generate Local Atomic Reactivity Indices from Gaussian16 log files*, v. 1.0; Santiago, Chile, 2020.

[51]. Gómez-Jeria, J. S. An empirical way to correct some drawbacks of Mulliken Population Analysis (Erratum in: J. Chil. Chem. Soc., 55, 4, IX, 2010). *Journal of the Chilean Chemical Society* **2009,** 54, 482-485.

[52]. Statsoft. *Statistica v.10*, 2300 East 14 th St. Tulsa, OK 74104, USA, 2011.